The Astrophysical Journal, 783:36 (7pp), 2014 March 1 doi:10.1088/0004-637X/783/1/36

AN OBSERVATIONAL INVESTIGATION OF THE IDENTITY OF B11244 (l–C_3H^+/C_3H^-)

Brett A. McGuire[1], P. Brandon Carroll[1], Pierre Gratier[2,3], Viviana Guzmán[2], Jerome Pety[2,3], Evelyne Roueff[4,5], Maryvonne Gerin[3], Geoffrey A. Blake[6], and Anthony J. Remijan[7]
[1] Division of Chemistry and Chemical Engineering, California Institute of Technology, Pasadena, CA 91125, USA
[2] IRAM, 300 rue de la Piscine, F-38406 Saint Martin d'Hères, France
[3] LERMA, UMR 8112, CNRS and Observatoire de Paris, 61 avenue de l'Observatoire, F-75014 Paris, France
[4] LUTH, UMR 8102, CNRS and Observatoire de Paris, Place J. Janssen, F-92195 Meudon Cedex, France
[5] LERMA, UMR 8112, CNRS and Observatoire de Paris, Place J. Janssen, F-92190, Meudon, France
[6] Division of Chemistry and Chemical Engineering and Division of Geological and Planetary Sciences, California Institute of Technology, Pasadena, CA 91125, USA
[7] National Radio Astronomy Observatory, Charlottesville, VA 22903, USA
Received 2013 October 11; accepted 2013 November 27; published 2014 February 11

ABSTRACT

Pety et al. have reported the detection of eight transitions of a closed-shell, linear molecule (B11244) in observations toward the Horsehead photodissociation region (PDR), which they attribute to the l–C_3H^+ cation. Recent high-level ab initio calculations have called this assignment into question; the anionic C_3H^- molecule has been suggested as a more likely candidate. Here, we examine observations of the Horsehead PDR, Sgr B2(N), TMC-1, and IRC+10216 in the context of both l–C_3H^+ and C_3H^-. We find no observational evidence of $K_a = 1$ lines, which should be present were the carrier indeed C_3H^-. Additionally, we find a strong anticorrelation between the presence of known molecular anions and B11244 in these regions. Finally, we discuss the formation and destruction chemistry of C_3H^- in the context of the physical conditions in the regions. Based on these results, we conclude there is little evidence to support the claim that the carrier is C_3H^-.

Key words: astrochemistry – ISM: clouds – ISM: individual objects (Sagittarius B2(N), TMC-1, Horsehead PDR, IRC+10216) – ISM: molecules

Online-only material: color figure, machine-readable table

1. INTRODUCTION

Pety et al. (2012) have reported the detection of eight transitions of a closed-shell, linear molecule in observations toward the Horsehead photodissociation region (PDR). They performed a spectroscopic analysis and fit to these transition frequencies and, based on comparison with theoretical work (see Ikuta 1997, and references therein), attribute these transitions to the l–C_3H^+ cation. Later, McGuire et al. (2013) identified the $J = 1$–0 and $J = 2$–1 transitions predicted by Pety et al. (2012) in absorption toward the Sgr B2(N) molecular cloud.

The cation l–C_3H^+ is important in the chemistry of hydrocarbons because reactions with it are thought to be the most important gas-phase channels to form other small hydrocarbons (Turner et al. 2000; Wakelam et al. 2010), like C_3H and C_3H_2, which are widely observed in different environments. However, the observed abundances of C_3H and C_3H_2 in PDRs are much higher than what pure gas-phase models predict. One possible explanation is that polycyclic aromatic hydrocarbons (PAHs) are fragmented into these small hydrocarbons in PDRs due to the strong UV fields (see e.g., Fuente et al. 2003; Teyssier et al. 2004; Pety et al. 2005). The discovery of l–C_3H^+ thus brings further constraints to the formation pathways of the small hydrocarbons in these environments.

The attribution of these signals to the l–C_3H^+ cation, however, has since been disputed by Huang et al. (2013) and Fortenberry et al. (2013), with the latter suggesting the anion C_3H^- as a more probable carrier based on high-level theoretical work. Because of the open question of identity, McGuire et al. (2013) used the convention of referring to the carrier as B11244, which we adopt here.

In this paper, we re-examine the observations of Pety et al. (2012) toward the Horsehead PDR, as well as PRebiotic Interstellar MOlecular Survey (PRIMOS) observations of Sgr B2(N), the Kaifu et al. (2004) survey of TMC-1, and the Barry E. Turner Legacy survey of IRC+10216 in the context of discussing: "What if B11244 is actually C_3H^-?" In Section 2, we discuss the spectroscopy of C_3H^- using the properties derived by Fortenberry et al. (2013) and present simulated spectra. In Section 3, we briefly outline the observations used and in Section 4 discuss the analysis of these observations. Finally, in Section 5 we present the results of our findings and discuss them in the context of determining the identity of B11244.

2. SPECTROSCOPIC ANALYSIS

Table 1 provides the rotational constants and dipole moments used in this work to describe B11244, assuming it is either l–C_3H^+ or C_3H^-. The spectroscopic constants and fit for l–C_3H^+ are provided in Pety et al. (2012), and their predictive power is confirmed in McGuire et al. (2013). Fortenberry et al. (2013) provide a high-accuracy equilibrium structure for C_3H^-, rotational constants, and dipole moments. These moments are not in the principal axis (PA) system but can readily be converted to the PA system with a simple coordinate rotation resulting in $\mu_x \rightarrow \mu_a = 1.63$ debye and $\mu_y \rightarrow \mu_b = 1.41$ debye. Indeed, the magnitude of this rotation is small, such the values of these dipole moments remain essentially unchanged. Assuming B11244 is C_3H^-, the observed transitions in Pety et al. (2012) and McGuire et al. (2013) are a-type, $K_a = 0$ transitions, and thus $(B+C)$ and D_J can be well determined from these lines. To obtain these constants, the observed transitions from Pety et al. (2012) and McGuire et al. (2013) were fit using the

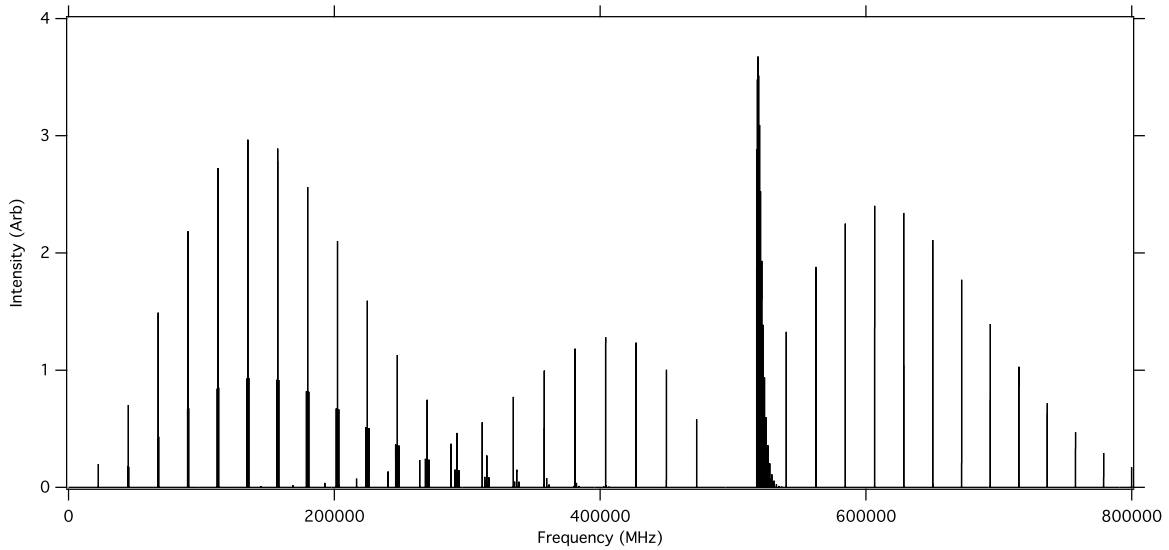

Figure 1. Simulated spectrum of C_3H^- at LTE, with an excitation temperature of $T_{ex} = 22$ K.

Table 1
Rotational Constants and Dipole Moments for B11244, Assuming it is *l*–C_3H^+ or C_3H^-

Constant	*l*–C_3H^+	References	C_3H^-	References
A (MHz)	...	...	529 134	(3)
B (MHz)	11 244.9512(15)	(2)	11 355.3	(1)
C (MHz)	...	...	11 134.5	(1)
D (kHz)	7.766(40)	(2)	...	...
D_J (kHz)	...	...	4.63	(1)
D_{JK} (kHz)	...	...	702	(3)
D_K (MHz)	...	...	218	(3)
d_1 (Hz)	...	...	−112	(3)
d_2 (Hz)	...	...	−23	(3)
H (Hz)	0.56(19)	(2)	...	...
μ_a (debye)	...	...	1.63	(1, 3)
μ_b (debye)	3	(2)	1.41	(1, 3)

References. (1) This work; (2) Pety et al. 2012; (3) Fortenberry et al. 2013.

Table 2
CALPGM Catalog Simulation of C_3H^- Format

Column	Format	Description
1	F13.4	Frequency (MHz)
2	F8.4	Error of Freq (MHz)
3	F8.4	Base 10 log intensity (nm^2MHz at 300 K)
4	I2	Degrees of freedom in partition function
5	F10.4	Lower state energy (cm^{-1})
6	I3	Upper state degeneracy
7	I7	Species tag
8	I4	Quantum number format identifier
9	6I2	Upper state quantum numbers
10	6I2	Lower state quantum numbers

Notes. For a complete description of this file format, see CALPGM documentation located at spec.jpl.nasa.gov.

(This table is available in its entirety in a machine-readable form in the online journal. A portion is shown here for guidance regarding its form and content.)

CALPGM suite of programs. An asymmetric-top Hamiltonian with a Watson S reduction in the I^r representation was used.[8] The remaining constants were necessarily used as is from the theoretical calculations. A simulated spectrum of C_3H^- at 22 K using this combined set of constants is displayed in Figure 1. A full CALPGM catalog for C_3H^- to 2 THz is also provided as Supplemental Information (see Table 2).

3. OBSERVATIONS

Sgr B2(N). The data presented toward Sgr B2(N) were obtained as part of the PRIMOS project using the Robert C. Byrd 100 m Green Bank Telescope. The observed position was at (J2000) $\alpha = 17^h47^m19\overset{s}{.}8$, $\delta = -28^\circ22'17''$. An LSR source velocity of +64 km s^{-1} was assumed. Full observational details, including data reduction procedures and analysis, are given in Neill et al. (2012a).[9]

IRC+10216. The observations presented toward IRC+10216 are part of the Barry E. Turner Legacy Survey using the NRAO 12 m telescope on Kitt Peak. The observed position was at (J2000) $\alpha = 9^h47^m57\overset{s}{.}3$, $\delta = +13^\circ16'43''$. An LSR source velocity of −26 km s^{-1} was assumed. Full observational details are given in Remijan et al. (2008).[10]

TMC-1. The observations presented toward the TMC-1 dark cloud were taken as part of the Kaifu et al. (2004) survey using the Nobeyama Radio Observatory 45 m telescope. The observed position was at (J2000) $\alpha = 4^h41^m42\overset{s}{.}5$, $\delta = +25^\circ41'26\overset{''}{.}9$. An LSR source velocity of +5.85 km s^{-1} was assumed. Full observational details are given in Kaifu et al. (2004).

Horsehead PDR. The observations presented toward the Horsehead PDR were taken with the IRAM 30 m telescope as part of the Horsehead WHISPER project (PI: J. Pety). The observed position was at (J2000) $\alpha = 5^h40^m53\overset{s}{.}936$, $\delta = -2^\circ28'00''$. An LSR source velocity of +10.7 km s^{-1} was assumed. Full observational details are given in Pety et al. (2012).

[8] Full details on the expressions and algorithms can be found in the CALPGM documentation and references therein. The interested reader may find that the analytical analysis presented by Polo (1957) provides a useful (and more approachable) approximation.

[9] Access to the entire PRIMOS data set, specifics on the observing strategy, and overall frequency coverage information is available at http://www.cv.nrao.edu/~aremijan/PRIMOS/.

[10] All observations from the PRIMOS project and Barry E. Turner Legacy Survey are accessible at http://www.cv.nrao.edu/~aremijan/SLiSE.

Table 3
Observed and Targeted Transitions of B11244, Assuming it is C_3H^-

Transition	ν	S_{ij}	E_u	Horsehead		Sgr B2(N)		IRC+10216	
$J'_{K_a,K_c} - J''_{K_a,K_c}$	(MHz)		(K)	ΔT_{mb}	ΔV	ΔT_A^*	ΔV	ΔT_A^*	ΔV
$1_{0,1} \rightarrow 0_{0,0}$	22 489.86	1	1.079	...	...	−27	13.4	...	...
$2_{1,2} \rightarrow 1_{1,1}$	44 755.94	1.5	28.07	...	...	[a]	14.7	...	...
$2_{0,2} \rightarrow 1_{0,1}$	44 979.50	2	3.237	...	...	−70	14.7	...	...
$2_{1,1} \rightarrow 1_{1,0}$	45 197.57	1.5	28.10	...	...	⩽9	14.7	...	...
$4_{1,4} \rightarrow 3_{1,3}$	89 510.82	3.75	35.59	⩽5.7	0.81	...	...	...	...
$4_{0,4} \rightarrow 3_{0,3}$	89 957.63	4	10.79	89	0.81	...	...	...	...
$4_{1,3} \rightarrow 3_{1,2}$	90 394.13	3.75	35.70	⩽5.3	0.81	...	...	...	...
$5_{1,5} \rightarrow 4_{1,4}$	111 887.54	4.8	40.96	⩽10.5	0.81	...	...	...	...
$5_{0,5} \rightarrow 4_{0,4}$	112 445.57	5	16.19	115	0.81	...	...	...	...
$5_{1,4} \rightarrow 4_{1,3}$	112 991.72	4.8	41.11	⩽14.1	0.81	...	...	...	...
$6_{0,6} \rightarrow 5_{0,5}$	134 932.69	6	22.66	72	0.81	⩽52	13	⩽5	27.5
$7_{0,7} \rightarrow 6_{0,6}$	157 418.71	7	30.22	75	0.81	99[b]	13	⩽7	27.5
$9_{0,9} \rightarrow 8_{0,8}$	202 386.75	9	48.56	62	0.81	...	...	...	...
$10_{0,10} \rightarrow 9_{0,9}$	224 868.40	10	59.36	30	0.81	...	...	...	...
$11_{0,11} \rightarrow 10_{0,10}$	247 348.23	11	71.23	45	0.81	...	...	...	...
$12_{0,12} \rightarrow 11_{0,11}$	269 826.05	12	84.18	25	0.81	...	...	...	...

Notes. For simplicity, only those $K_a = 1$ transitions specifically searched for in our study are displayed. ΔT_A^* and ΔT_{mb} given in units of mK, ΔV given in units of km s^{-1}. All upper limits are 1σ. Values for the Horsehead PDR and Sgr B2(N) are based on Gaussian fits to the line shapes. The FWHM for IRC+10216 is based on a zeroth-order approximation from other observed transitions.
[a] Completely obscured by blends.
[b] Partially blended.

4. DATA ANALYSIS

The column density of B11244 in each source, assuming local thermodynamic equilibrium (LTE), can be calculated using

$$N_T = \frac{3k}{8\pi^3} \times \frac{Q_r e^{E_u/T_{ex}}}{\nu S\mu^2} \times \frac{\sqrt{\pi}}{2ln2} \times \frac{\Delta T_A^* \Delta V/\eta_b}{1 - \frac{(e^{h\nu/kT_{ex}}-1)}{(e^{h\nu/kT_{bg}}-1)}} \text{ cm}^{-2}, \quad (1)$$

following the convention of Hollis et al. (2004).

Here, N_T is the total column density, Q_r is the rotational partition function, E_u is the upper state energy, T_{ex} is the excitation temperature, ν is the frequency of the transition, $S\mu^2$ is the transition strength, ΔT_A^* is the peak line intensity, ΔV is the line FWHM, η_b is the beam efficiency at frequency ν, and T_{bg} is the background temperature.

In the case of l–C_3H^+, the partition function is well approximated by the standard linear-molecule formula given by

$$Q_r(l\text{–}C_3H^+) \approxeq \frac{kT}{hB} = 1.85(T), \quad (2)$$

with B expressed in Hz. For C_3H^-, the following equation is appropriate (Gordy & Cook 1984):

$$Q_r(C_3H^-) \approxeq \frac{5.34 \times 10^6}{\sigma} \left(\frac{T^3}{ABC}\right)^{1/2} = 0.65(T_{ex})^{3/2}, \quad (3)$$

with $\sigma = 1$ and rotational constants with units of MHz. The accuracy of Q_r for the anion is dependent on the accuracy of the rotational constants used. Thus, there is likely an uncertainty of a few percent in the value of Q_r used here. In any case, the partition function for the anion rapidly outpaces that of the cation above $T_{ex} \sim 8$ K.

To calculate upper limits of l–C_3H^+ in IRC+10216, we use the molecule-specific parameters given in McGuire et al. (2013) and the upper limit ΔT_A^* and ΔV values given in Table 3. The line parameters and molecule-specific parameters used for all C_3H^- calculations are given in Table 3.

While the observed $K_a = 0$ transitions allow us to constrain B and C reasonably well, the lack of any confirmed detection of a $K_a = 1$ transition limits the overall accuracy in predicting the frequencies of these lines. However, the expected intensity of these lines, given a derived column density and temperature, is likely to be fairly accurate under LTE conditions. In the Horsehead PDR, these lines should have a peak intensity of $T_{mb} \sim$ 20–28 mK for $J'' =$ 3–6, using the derived conditions from the $K_a = 0$ transitions. In Sgr B2(N), the expected intensities are below the detectable values in our observations.

We calculate a theoretical uncertainty in the center frequencies for these transitions of $\sigma \sim 370$ MHz for the $J =$ 4–3 transition to as much as $\sigma \sim 650$ MHz for the $J =$ 7–6 transition. At LTE, the strongest of these lines fall within the 3 mm window of the Pety et al. (2012) survey. Due to the uncertainties in the line centers, we have searched a region equal to each transition's uncertainty on either side of each predicted line center. After identifying all known lines within this range, we find no detection of any signals which could be assigned to a $K_a = 1$ transition of C_3H^- at the rms noise level of the observations (∼5–10 mK), despite peak predicted intensities of 20–28 mK at LTE. An example spectrum of the region searched around the predicted $4_{1,4}$–$3_{1,3}$ transition is shown in Figure 2.

At higher frequencies ($\nu >$ 500 GHz), additional branches of C_3H^- transitions are predicted, with slightly greater intensity; we have no spectral coverage at these frequencies. However, these transitions are strongly dependent on the derived value for A, making any attempted search quite challenging.

5. RESULTS AND DISCUSSION

In the following paragraphs, we discuss the results of our analysis in the context of determining the identity of B11244. We do not address topics that have been previously covered in the literature and for which our analysis provides no further information. Namely, the agreement (or lack thereof) between the fitted rotational and distortion constants for each species

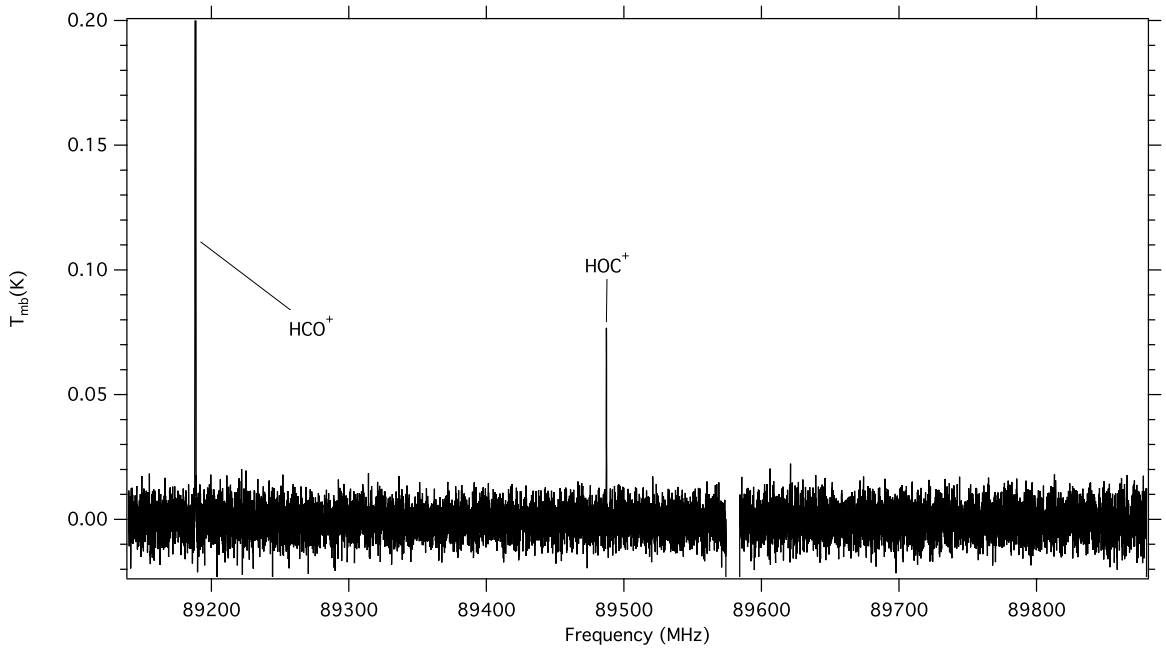

Figure 2. Targeted frequency window around the predicted $K_a = 1$, $4_{1,4}$–$3_{1,3}$ transition of C_3H^- centered at 89535 MHz. The rms noise level is 5.8 mK. Three features are observed, two of which are attributed to HCO^+ and HOC^+. A third, located at ~89580 MHz, has been positively identified as belonging to a known interstellar species, but has been removed from the spectra for proprietary reasons. The identity of this line will be published in a forthcoming paper from Guzmán et al.

Table 4
Column Densities and Excitation Temperatures for $l-C_3H^+$ and C_3H^- in our Observations and from the Literature as well as Ratios of These to Their Neutral Counterparts

	l–C_3H^+		C_3H^-		C_3H	l–C_3H^+/C_3H	C_3H^-/C_3H	C_6H^-/C_6H
Source	$N(10^{11}$ cm$^{-1})$	T_{ex}(K)	$N(10^{11}$ cm$^{-1})$	T_{ex}(K)	$N(10^{11}$ cm$^{-1})$	(%)	(%)	(%)
Horsehead PDR	4.8(9)[(1)]	14(2)[(1)]	12(1)[a]	22(4)[a]	21(7)[(1)]	23(3)	57(16)	$\leqslant$9
Sgr B2(N)	240(30)[b]	8[b]	790(90)[b]	8[b]	3000 (300)[b]	8(1)	26(8)	. . . [c]
IRC+10216	$\leqslant$6	32	$\leqslant$40	32	560	$\leqslant$1.1	$\leqslant$7.1	3(2)[(2)]
TMC-1	$\leqslant$6[d]	9	$\leqslant$250[d]	9	90[(3)]	$\leqslant$7	$\leqslant$278	2.5(0.4)[(4)]

Notes. Literature values for the ratio of C_6H^- to neutral C_6H are also shown. Uncertainties are given in parentheses in units of the last significant digit and are 1σ. All values were calculated for this work unless otherwise noted.
[a] To ensure consistency with the l–C_3H^+ values determined by Pety et al. (2012), these values have been determined via a rotation diagram analysis. A least-squares-fit analysis suggests this column density may actually be a factor of two higher.
[b] These values are slightly revised from those in McGuire et al. (2013). While re-examining the data for this study, it became clear that the transition at 45 GHz, regardless of the carrier, is likely highly subthermal. We therefore base our figures here on only the 22.5 GHz transition and assume the "standard" 8 K excitation temperatures for cold molecules in this source. We have extended this temperature to our previous analysis of C_3H in this source as well.
[c] There have been no reported detections of, and we see no evidence for, the presence of C_6H^- in Sgr B2(N).
[d] Based on a tentative detection of only the 45 GHz transition, which, like H_2CO, displays anomalous absorption against the 2.7 K CMB in this source.
References. (1) Pety et al. 2012; (2) McCarthy et al. 2006; (3) Kaifu et al. 2004; (4) Cordiner et al. 2013.

with those calculated by Huang et al. (2013) and Fortenberry et al. (2013).

5.1. Anion/Neutral Abundance Ratio

The results of fits to column density and excitation temperature in the Horsehead PDR and Sgr B2(N), and upper limits in IRC+10216 and TMC-1, are displayed in Table 4 for l–C_3H^+, C_3H^-, and C_6H^- as well as neutral C_3H and C_6H. In the Horsehead PDR and Sgr B2(N), the calculated column density for C_3H^- is ~3 times that of the cation. This is due to an increase in the partition function and a decrease in the value of $S_{ij}\mu^2$ for the anion.

Among the reported carbon-chain anionic species detected to date in the interstellar medium (ISM; C_4H^-, C_6H^-, C_8H^-), C_6H^- has been the most widely detected and characterized (Gupta et al. 2009; Cordiner et al. 2013). The abundance fraction of C_6H^-, relative to the neutral species, is remarkably consistent across observed sources, varying from ~1.4% to 4.4% (Cordiner et al. 2013; McCarthy et al. 2006). The abundance ratio of C_3H^- to neutral C_3H, which is more than an order of magnitude greater than that of C_6H^- in observed sources, is therefore somewhat surprising. Additionally puzzling is that C_3H^- appears to break the observed trend of increasing anion abundance fraction with increasing size as well as the apparent trend for even-carbon molecular anions.

Fortenberry et al. (2013) proposed the most likely route to efficient formation of C_3H^- is through a radiative attachment (RA) mechanism. Herbst & Osamura (2008) calculated an exceptionally low RA rate for C_3H. At 300 K, they found an

attachment rate for C_3H orders of magnitude lower than for C_4H, C_6H, and C_8H. Despite this, if B11244 is indeed C_3H^-, it would be the highest anion/neutral ratio detected in the ISM.[11]

As described by Fortenberry et al. (2013), C_3H^- possesses both dipole-bound and valence-excited states of the same multiplicity, which provide the necessary states to allow for an RA mechanism to form the anion (Güthe et al. 2001; Carelli et al. 2013). Because the other detected anions possess only a dipole-bound state, Fortenberry et al. (2013) proposed that the presence of the valence excited state may cause an enhancement in the production of C_3H. The extent of this enhancement is difficult to quantify, and thus we cannot say whether this can offset the lower RA rate predicted by Herbst & Osamura (2008).

5.2. Detection in Sgr B2(N)

To our knowledge, no molecular anions have been detected in Sgr B2(N). An examination of both the PRIMOS centimeter-wave data and the 2 mm Turner Survey shows no indication of the presence of any of the known molecular anions. Of note, no such anions have been detected in the Horsehead PDR either (Agúndez et al. 2008).

However, a re-examination of the PRIMOS data originally presented in McGuire et al. (2013) finds some evidence for B11244 absorption in lower-velocity ($V_{LSR} \sim$ +0–10 km s^{-1} and $V_{LSR} \sim$ +18 km s^{-1}) diffuse clouds along the line of sight to Sgr B2(N). For illustration, the $J = 1$–0 and $J = 2$–1 transitions of B11244 are shown in Figure 3 in comparison to the known CH absorption spectra toward SgrB2(N).[12] The strongest observed transition of l–C_3H is also shown and displays low-velocity absorption as well, although the ∼0 km s^{-1} component is blended with the +64 km s^{-1} main component of the l–C_3H, $J = 3/2 - 1/2$, f-parity, $F = 1$–0 transition.

While numerous cationic species have been detected in these diffuse clouds (see e.g., Gerin et al. 2010 & Godard et al. 2010), the possibility of anion chemistry in these regions is not well understood. Indeed, no anions have previously been seen in these line-of-sight clouds. The indication of B11244 in these regions, presented here, will hopefully be a motivating factor that will drive future studies. Investigations of this diffuse gas, which displays chemistry distinct from regions such as IRC+10216 and Sgr B2(N), will certainly prove invaluable in furthering our understanding of gas-phase ion chemistry.

5.3. Nondetection in IRC+10216

IRC+10216 has been the preeminent source for the detection of anionic species. The carbon-chain anions C_4H^-, C_6H^-, and C_8H^- have all been detected in this source (Gupta et al. 2007; Cernicharo et al. 2007; McCarthy et al. 2006; Remijan et al. 2007) as well as the cyano-anions CN^-, C_3N^-, and C_5N^- (Agúndez et al. 2010; Thaddeus et al. 2008; Cernicharo et al. 2008). As shown in Table 3, however, we see no signal from B11244 toward this source at an rms of ∼5–7 mK. Given the known abundance of the neutral C_3H, we can determine upper limits to the anion fraction. We assume a rotational temperature of 32 K—similar to that of C_6H^- and C_8H^- in this source and slightly higher than that of C_4H^-. This results in an upper limit abundance fraction for C_3H^-/C_3H of only ∼7% (see Table 4), which is about twice that of C_6H^- and less than half of the lower edge of our error bars in Sgr B2(N).

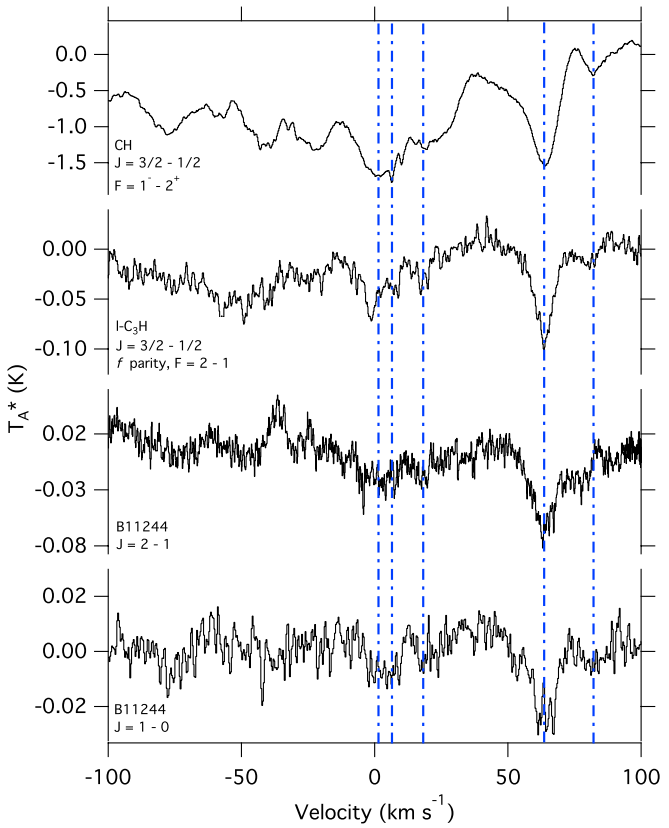

Figure 3. Observed transitions of B11244 and l–C_3H toward Sgr B2(N) from PRIMOS and CH toward Sgr B2(N) from HEXOS. The blue vertical lines are provided to guide the eye to the diffuse cloud velocity components. The velocity axis is referenced to the rest frequency of each transition.

(A color version of this figure is available in the online journal.)

5.4. Anion Destruction via Photodetachment

Kumar et al. (2013) have recently shown that UV photodetachment may be the dominant destruction mechanism of interstellar anions in IRC+10216. Their models assume the standard interstellar UV radiation field (cf. Draine 1978) and find UV photodetachment is significant at these values. In the Horsehead PDR, however, the UV field is ∼60 times the standard UV value (Habart et al. 2005). It is therefore contradictory that despite a far higher (destructive) UV field, C_3H^- would be present in the Horsehead PDR with an anion–neutral ratio eight times higher than the upper limit for IRC+10216.

5.5. Non-detection of $K_a = 1$ Transitions

The lack of detection of any signal that could reasonably be attributed to emission from $K_a = 1$ transitions strongly disfavors the assignment of B11244 to C_3H^-. In the Horsehead PDR, the $K_a = 0$ transitions of B11244 are well modeled by LTE assumptions, and thus we do expect the intensity of the $K_a = 1$ transitions to be reasonably well predicted. It should be noted, however, that a single molecule can display distinctly different excitation temperatures and column densities between two K ladders. Indeed, previous observations of HNCO toward OMC-1 show distinct differences between LTE column density and temperature measurements in high-K and low-K ladders (Blake et al. 1987). The authors attribute this to radiative

[11] Cernicharo et al. 2008 found an abundance ratio of C_5N^-/C_5N in IRC+10216 of 57%, but suggested it may in fact be as low as 12.5%.

[12] The CH spectra shown are from the HEXOS survey of Sgr B2(N). Full observation, reduction, and analysis details are available in Neill et al. (2012b) and Neill et al. (2014).

excitation of the higher-K, higher-energy states through strongly allowed b-type transitions at far-infrared (far-IR) wavelengths.

In the case of C_3H^-, we can examine three limiting cases which may apply in the Horsehead PDR: LTE conditions, the influence of a weak far-IR radiation field, and the influence of a strong far-IR radiation field.

5.5.1. LTE

As shown in Section 4, under LTE conditions the $K_a = 1$ transitions of C_3H^- have predicted intensities of 20–28 mK. These are clearly not detected in our spectra at the rms noise level of the observations (∼5–10 mK). Thus we can say with some certainty that C_3H^- is not present in the Horsehead PDR under LTE conditions.

5.5.2. Weak far-IR radiation field

In the case of a weak far-IR radiation field, and assuming low to moderate H_2 densities in the region (i.e., non-LTE), the population of the $K_a = 1, 2, \ldots$ levels will be largely dominated by radiative selection rules. Any population driven into the $K_a = 1, 2, \ldots$ levels by collisions will rapidly decay back into the $K_a = 0$ states via radiative emission. For C_3H^-, this will result in a decrease in the observed intensity of the $K_a = 1$ transitions, relative to the $K_a = 0$ transitions, as compared to LTE. In this case, the lack of detected $K_a = 1$ transitions does not provide a constraint on the presence of C_3H^-.

5.5.3. Strong Far-IR Radiation Field

We now examine the case of a strong far-IR radiation field and low to moderate H_2 densities in the region (i.e., non-LTE). For transitions arising from low-energy states, the relative populations will be determined by the rotational excitation temperature of the molecule ($T_{ex} = 22$ K). For transitions from higher-energy states connected by far-IR transitions, the relative populations of the energy levels will be determined by the color temperature of the dust-radiation field at that frequency if that temperature is higher than T_{ex}. Thus, the $K_a = 1, 2, \ldots$ transitions would be relatively more intense than predicted by LTE simulations at T_{ex}. This is the case for HNCO in OMC-1 (Blake et al. 1987), where the higher-K transitions are more intense than predicted from observations of the lower-K transitions.

In the Horsehead PDR, Goicoechea et al. (2009) measured the millimeter dust continuum to have a temperature $T_d \simeq 30$ K. Under these circumstances, we would expect the $K_a = 1$ transitions to have intensities of ∼27–34 mK. We can therefore conclude that, assuming B11244 is subject to the radiation field measured by Goicoechea, C_3H^- is not the carrier.

It is clear from the two non-LTE cases discussed above that the location of B11244 within the Horsehead PDR region is critical. Interferometric mapping of the location of B11244, relative to the measured continuum levels in this region, will provide considerable insight into the mechanisms at work.

6. CONCLUSIONS

We have presented an analysis of observations of the Horsehead PDR, Sgr B2(N), IRC+10216, and TMC-1 with the goal of determining the identity of B11244. Our findings can be summarized as follows:

1. If B11244 is C_3H^-, it would display the highest anion–neutral ratio yet observed in the ISM (57% in the Horsehead PDR).
2. We find no evidence for C_3H^- emission in observations toward IRC+10216 and place an upper limit on the anion–neutral ratio in this source well below that found in the Horsehead PDR and Sgr B2(N).
3. Recent work has shown UV photodetachment is a dominant destruction pathway for molecular anions (Kumar et al. 2013). Despite a UV field more than 60 times that of IRC+10216, C_3H^- would be present in the Horsehead PDR with an anion–neutral ratio more than eight times that of the upper limit in IRC+10216.
4. We find no evidence for the $K_a = 1$ lines of C_3H^- in observations of the Horsehead PDR. We examine three limiting cases for conditions within the Horsehead PDR and find that a weak far-IR radiation field can account for the lack of observed $K_a = 1$ transitions. LTE conditions or the presence of a strong far-IR radiation field, however, strongly disfavor the presence of C_3H^-. A significant far-IR radiation field has been reported for the Horsehead PDR, but it is unclear whether B11244 is subject to this radiation.

The observational evidence presented here, taken as a whole, casts doubt on the assignment of B11244 to C_3H^-, favoring instead the cation l–C_3H^+ as the most likely candidate. The evidence is, however, circumstantial; a definitive answer will almost certainly require laboratory confirmation. Indeed, K.N. Crabtree and coworkers at the Harvard-Smithsonian Center for Astrophysics have undertaken such work using Fourier-transform microwave spectroscopy. Preliminary evidence is suggestive of the cationic species. The full results of the laboratory investigation will be published in an upcoming paper (K.N. Crabtree 2013, private communication).

Additional observations of the Horsehead PDR, with the aim of detecting the b-type transitions of C_3H^-, predicted to be strongest between 500–600 GHz, would also provide further evidence. Perhaps more insightful would be interferometric observations to discover the spatial correlation, or lack thereof, of B11244 with the previously observed far-IR radiation field. Finally, further observations of the diffuse gas along the sightline to Sgr B2(N) would likely prove fruitful in understanding the possibility of anion chemistry in these regions.

We are grateful to the anonymous referee for helpful comments which have greatly improved the quality of this manuscript. We thank E.A. Bergin and J.T. Neill for providing the HEXOS spectra presented here and M. Ohishi for providing the observational data toward TMC-1. We also thank H. Gupta, M. Cordiner, and A. Faure for insightful conversations. B.A.M. gratefully acknowledges funding by an NSF Graduate Research Fellowship. V.G. thanks support from the Chilean Government through the Becas Chile scholarship program. This work was partially funded by grant ANR-09-BLAN-0231-01 from the French Agence Nationale de la Recherche as part of the SCHISM project. The National Radio Astronomy Observatory is a facility of the National Science Foundation operated under cooperative agreement by Associated Universities, Inc.

REFERENCES

Agúndez, M., Cernicharo, J., Guélin, M., et al. 2008, A&A, 478, L19
Agúndez, M., Cernicharo, J., Guélin, M., et al. 2010, A&A, 517, L2
Blake, G. A., Sutton, E. C., Masson, C. R., & Phillips, T. G. 1987, ApJ, 315, 621
Carelli, F., Grassi, T., Sebastianelli, F., & Gianturco, F. A. 2013, MNRAS, 428, 1181

Cernicharo, J., Guélin, M., Agúndez, M., McCarthy, M. C., & Thaddeus, P. 2008, ApJL, 688, L83
Cernicharo, J., Guélin, M., Agúndez, M., et al. 2007, A&A, 467, L37
Cordiner, M. A., Buckle, J. V., Wirström, E. S., Olofsson, A. O. H., & Charnley, S. B. 2013, ApJ, 770, 48
Draine, B. T. 1978, ApJS, 36, 595
Fortenberry, R. C., Huang, X., Crawford, T. C., & Lee, T. J. 2013, ApJ, 772, 39
Fuente, A., Rodríguez-Franco, A., García-Burillo, S., Martín-Pintado, J., & Black, J. H. 2003, A&A, 406, 899
Gerin, M., De Luca, M., Black, J., et al. 2010, A&A, 518, L110
Godard, B., Falgarone, E., Gerin, M., Hily-Blant, P., & De Luca, M. 2010, A&A, 520, A20
Goicoechea, J. R., Compiègne, M., & Habart, E. 2009, ApJL, 699, L165
Gordy, W., & Cook, R. L. 1984, Microwave Molecular Spectra, Techniques of Chemistry, Vol. 18 (2nd ed; New York: Wiley)
Gupta, H., Brünken, S., Tamassia, F., et al. 2007, ApJL, 655, L57
Gupta, H., Gottlieb, C. A., McCarthy, M. C., & Thaddeus, P. 2009, ApJ, 691, 1494
Güthe, F., Tulej, M., Pachkov, M. V., & Maier, J. P. 2001, ApJ, 555, 466
Habart, E., Abergel, A., Walmsley, C. M., Teyssier, D., & Pety, J. 2005, A&A, 437, 177
Herbst, E., & Osamura, Y. 2008, ApJ, 679, 1670
Hollis, J. M., Jewell, P. R., Lovas, F. J., & Remijan, A. J. 2004, ApJL, 613, L45
Huang, X., Fortenberry, R. C., & Lee, T. J. 2013, ApJL, 768, L25
Ikuta, S. 1997, JChPh, 106, 4536
Kaifu, N., Ohishi, M., Kawaguchi, K., et al. 2004, PASJ, 56, 69
Kumar, S. S., Hauser, D., Jindra, R., et al. 2013, ApJ, 776, 25
McCarthy, M. C., Gottlieb, C. A., Gupta, H., & Thaddeus, P. 2006, ApJL, 652, L141
McGuire, B. A., Carroll, P. B., Loomis, R. A., et al. 2013, ApJ, 774, 56
Neill, J. T., Bergin, E. A., Lis, D. C., et al. 2012a, JMoSp, 280, 150
Neill, J. T., Bergin, E. A., Lis, D. C., et al. 2014, ApJ, in press
Neill, J. T., Muckle, M. T., Zaleski, D. P., et al. 2012b, ApJ, 755, 153
Pety, J., Gratier, P., Guzmàn, V., et al. 2012, A&A, 548, A68
Pety, J., Teyssier, D., Fossé, D., et al. 2005, A&A, 435, 885
Polo, S. R. 1957, CaJPh, 35, 880
Remijan, A. J., Hollis, J. M., Lovas, F. J., et al. 2007, ApJL, 664, L47
Remijan, A. J., Leigh, D. P., Markwick-Kemper, A. J., & Turner, B. E. 2008, arXiv:0802.2273v1
Teyssier, D., Fossé, D., Gerin, M., et al. 2004, A&A, 417, 135
Thaddeus, P., Gottlieb, C. A., Gupta, H., et al. 2008, ApJ, 677, 1132
Turner, B. E., Herbst, E., & Terzieva, R. 2000, ApJS, 126, 427
Wakelam, V., Smith, I. W. M., Herbst, E., et al. 2010, SSRv, 156, 13